Optimizing the performance of TOAD by changing the wavelength and power of control pulse

Liangsheng Wen (温亮生), Peng Zuo (左 鹏), Jian Wu (伍 剑), and Jintong Lin (林金桐)

Optical Center, Beijing University of Posts and Telecommunications, Beijing 100876

Received April 24, 2003

The performance of terahertz optical asymmetric demultiplexer (TOAD) has been studied by modelling the semiconductor optical amplifier (SOA) in which the intraband effects had been taken into account. Numerical results are coincident with the experiment results. We interpret why there are three peaks in the switching window, which has never been reported before. In addition, we put forward the definition of the flatness of the switching window of TOAD for the first time By analysing the different phase of clockwise and counter clockwise signal pulse changed by SOA, appropriate peak power of control pulse and wavelength of signal and control pulse have been calculated in order to obtain large output power and flat switching window of TOAD.

OCIS codes: 060.2330, 230.1150, 320.7110, 140.4480.

In recent years, terahertz optical asymmetric demultiplexers (TOADs) have become one of the key components in optical communication due to their many excellent features[1−3]. TOAD can be applied to demultiplex single channel signal in high speed optical time division multiplexing (OTDM) system. Furthermore, they can be used as intensity thresholding devices for clock recovery[4], as well as for bit self-synchronization when combined with optical phase-lock loop[5]. In optical packet switching networks based on OTDM, TOAD can also be used for address identifying and packet routing[6,7].

Generally, when the duration of pulse is smaller than 10 ps, not only the traditional nonlinear gain compress effects, but also the nonlinear gain compress caused by intraband effects, such as carrier heating (CH), spectral hole burning (SHB), two-photon absorption (TPA) and ultrafast nonlinear refraction (UNR) in semiconductor optical amplifier (SOA) should be taken into account. Several research groups have undertaken the theoretical and experimental studies[8,9]. Results show that there are two peaks in the heading and tailing part of the switching window respectively.

In this paper, the performance of TOAD is studied by modelling the SOA by taking into account the intraband effects. Numerical results are largely coincident with the experiment results. The interpretation on why there are three peaks in the switching window is given, which has never been reported before. We also point out the optimizing value of parameters such as the wavelengths and power of control and signal pulse in the two different applications of TOAD by analyze the flatness of switching window and the chirp property of output signal pulse. Results show that flat switching window and small chirped output signal pulse can be achieved by choosing appropriate power of control pulse and wavelength of signal and control pulse.

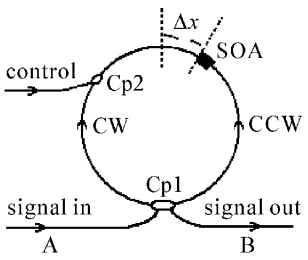

Fig. 1. Configuration of TOAD.

TOAD, as shown schematically in Fig. 1, is one kind of optical fiber loop devices. SOA acts as nonlinear medium, which is placed asymmetrically in the fiber loop. When the control pulse enters into the loop, because the SOA is offset from the middle point of the loop, the counter clockwise (CCW) pulse arrives to the SOA a little bit earlier than the control pulse while the opposite happens to the clockwise (CW) pulse. So the gain and phase of these two signal pulses are different. The two pulses interfered with each other when they arrived at coupler1 (Cp1). Then the signal pulse comes out from port B if the difference of phase changing between the clockwise and counter clockwise signal pulse is the odd times of π. By change the offset Δx from the midpoint of the loop, the different switching window is obtained.

Details of the theoretical model taking into account intraband effects are printed in Refs. [10] and [11]. The summary lines are described as

$$\frac{\partial A_{\rm ctr}}{\partial z} = \frac{1}{2}\frac{G_{\rm ctr}-\varepsilon_2 P_{\rm ctr}^2}{1+\varepsilon_1 P_{\rm ctr}^2}A_{\rm ctr} - \frac{i}{2}\left(\alpha_{\rm N}G_{\rm ctr} - \alpha_{\rm T}\frac{\varepsilon_1 G_{\rm ctr}P_{\rm ctr}+\varepsilon_2 P_{\rm ctr}^2}{1+\varepsilon_1 P_{\rm ctr}^2}\right)A_{\rm ctr} - \left(\Gamma_2\beta_2 + i\Gamma_2'\frac{\omega_{0\_\rm ctr}}{C}n_2\right)\frac{1}{\sigma}A_{\rm ctr}P_{\rm ctr} - \frac{1}{2}\alpha_{\rm int}A_{\rm ctr}, \tag{1}$$

$$\frac{\partial A_{\rm sgl}}{\partial z} = \frac{1}{2}\frac{G_{\rm sgl}-\varepsilon_2 P_{\rm ctr}^2}{1+\varepsilon_1 P_{\rm ctr}^2}A_{\rm sgl} - \frac{i}{2}\left(\alpha_{\rm N}G_{\rm sgl} - \alpha_{\rm T}\frac{\varepsilon_1 G_{\rm sgl}P_{\rm ctr}+\varepsilon_2 P_{\rm ctr}^2}{1+\varepsilon_1 P_{\rm ctr}^2}\right)A_{\rm sgl} - \left(\Gamma_2\beta_2 + i\Gamma_2'\frac{\omega_{0\_\rm sgl}}{C}n_2\right)\frac{1}{\sigma}A_{\rm sgl}P_{\rm ctr} - \frac{1}{2}\alpha_{\rm int}A_{\rm sgl} - \frac{1}{2}\eta_{\rm ctr\_sgl}P_{\rm cw}A_{\rm sgl}. \tag{2}$$

The equations for gain are

$$\frac{\partial G_{\rm ctr}}{\partial t} = \frac{G_{\rm s\_ctr} - G_{\rm ctr}}{\tau_{\rm s}} - \frac{1}{E_{\rm s\_ctr}} \frac{G_{\rm ctr} - \varepsilon_2 P_{\rm ctr}^2}{1 + \varepsilon_1 P_{\rm ctr}} P_{\rm ctr} + \Gamma_2 \beta'_{2\_\rm ctr} P_{\rm ctr}^2, \quad (3)$$

$$\frac{\partial G_{\rm sgl}}{\partial t} = \frac{G_{\rm s\_sgl} - G_{\rm sgl}}{\tau_{\rm s}} - \frac{1}{E_{\rm s\_sgl}} \frac{G_{\rm ctr} - \varepsilon_2 P_{\rm ctr}^2}{1 + \varepsilon_1 P_{\rm ctr}} P_{\rm ctr} + \Gamma_2 \beta'_{2\_\rm sgl} P_{\rm ctr}^2. \quad (4)$$

where A is the slowly varying envelope of field, subscript sgl can be CW and CCW. Let $A = \sqrt{P}\mathrm{e}^{i\phi}$, and substitute it into Eqs. (1)−(4), where P and ϕ are the power and phase. Then we can get

$$\begin{cases} \frac{\partial P_{\rm ctr}}{\partial z} = \frac{G_{\rm ctr} - \varepsilon_2 P_{\rm ctr}^2}{1 + \varepsilon_1 P_{\rm ctr}} P_{\rm ctr} - 2\Gamma_2 \beta_2 \frac{1}{\sigma} P_{\rm ctr} - \alpha_{\rm int} P_{\rm ctr} \\ \frac{\partial \phi_{\rm ctr}}{\partial z} = -\frac{1}{2}\left(\alpha_{\rm N} G_{\rm ctr} - \alpha_{\rm T} \frac{\varepsilon_1 G_{\rm ctr} P_{\rm ctr} + \varepsilon_2 P_{\rm ctr}^2}{1 + \varepsilon_1 P_{\rm ctr}}\right) - \Gamma'_2 \frac{\omega_{0\_\rm ctr}}{C} n_2 \frac{1}{\sigma} P_{\rm ctr} \\ \frac{\partial G_{\rm ctr}}{\partial t} = \frac{G_{\rm s0} - G_{\rm ctr}}{\tau_{\rm s}} - \frac{1}{E_{\rm s\_ctr}} \frac{G_{\rm ctr} - \varepsilon_2 P_{\rm ctr}^2}{1 + \varepsilon_1 P_{\rm ctr}} P_{\rm ctr} + \Gamma_2 \beta'_{2\_\rm ctr} P_{\rm ctr}^2 \end{cases}, \quad (5)$$

$$\begin{cases} \frac{\partial P_{\rm cw}}{\partial z} = \frac{G_{\rm cw} - \varepsilon_2 P_{\rm ctr}^2}{1 + \varepsilon_1 P_{\rm ctr}} P_{\rm cw} - \alpha_{\rm int} P_{\rm cw} - \left[2\Gamma_2 \beta_2 \frac{1}{\sigma} + \mathrm{Real}(\eta_{\rm ctr\_sgl})\right] P_{\rm ctr} P_{\rm cw} \\ \frac{\partial \phi_{\rm cw}}{\partial z} = -\frac{1}{2}\left(\alpha_{\rm N} G_{\rm cw} - \alpha_{\rm T} \frac{\varepsilon_1 G_{\rm cw} P_{\rm ctr} + \varepsilon_2 P_{\rm ctr}^2}{1 + \varepsilon_1 P_{\rm ctr}}\right) - \left[\Gamma'_2 \frac{\omega_{0\_\rm sgl}}{C} n_2 \frac{1}{\sigma} + \frac{1}{2}\mathrm{Image}(\eta_{\rm ctr\_sgl})\right] P_{\rm ctr} \\ \frac{\partial G_{\rm cw}}{\partial t} = \frac{G_{\rm s\_sgl} - G_{\rm cw}}{\tau_{\rm s}} + \Gamma_2 \beta'_{2\_\rm sgl} P_{\rm ctr}^2 - \frac{1}{E_{\rm s\_sgl}} \frac{G_{\rm ctr} - \varepsilon_2 P_{\rm ctr}^2}{1 + \varepsilon_1 P_{\rm ctr}} P_{\rm ctr} \end{cases}, \quad (6)$$

$$\begin{cases} \frac{\partial P_{\rm ccw}}{\partial z} = \frac{G_{\rm ccw} - \varepsilon_2 P_{\rm ctr}^2}{1 + \varepsilon_1 P_{\rm ctr}} P_{\rm ccw} - \alpha_{\rm int} P_{\rm ccw} - \left[2\Gamma_2 \beta_2 \frac{1}{\sigma} + \mathrm{Real}(\eta_{\rm ctr\_sgl})\right] P_{\rm ctr} P_{\rm ccw} \\ \frac{\partial \phi_{\rm ccw}}{\partial z} = -\frac{1}{2}\left(\alpha_{\rm N} G_{\rm ccw} - \alpha_{\rm T} \frac{\varepsilon_1 G_{\rm ccw} P_{\rm ctr} + \varepsilon_2 P_{\rm ctr}^2}{1 + \varepsilon_1 P_{\rm ctr}}\right) - \left[\Gamma'_2 \frac{\omega_{0\_\rm sgl}}{C} n_2 \frac{1}{\sigma} + \frac{1}{2}\mathrm{Image}(\eta_{\rm ctr\_sgl})\right] P_{\rm ctr} \\ \frac{\partial G_{\rm ccw}}{\partial t} = \frac{G_{\rm s\_sgl} - G_{\rm ccw}}{\tau_{\rm s}} + \Gamma_2 \beta'_{2\_\rm sgl} P_{\rm ctr}^2 - \frac{1}{E_{\rm s\_sgl}} \frac{G_{\rm ctr} - \varepsilon_2 P_{\rm ctr}^2}{1 + \varepsilon_1 P_{\rm ctr}} P_{\rm ctr} \end{cases}, \quad (7)$$

where Real(x) means the real part of x, Image(x) means the imaginary part of x, and $\eta_{\rm ctr\_sgl}$ is the coupling coefficient describing the nonlinear interaction between control and signal pulse, which can be written as

$$\eta_{\rm ctr\_sgl} = \eta^{\rm CD}_{\rm ctr\_sgl} + \eta^{\rm CH}_{\rm ctr\_sgl} + \eta^{\rm SHB}_{\rm ctr\_sgl}, \quad (8)$$

where

$$\eta^{\rm CD}_{\rm ctr\_sgl} = \frac{g_{\rm s\_sgl} \alpha_{\rm sgl} \tau_{\rm s}}{\hbar \omega_{0\_\rm sgl} \sigma} (1 - i\alpha_{\rm N}) \times \frac{1}{[-i(\omega_{0\_\rm ctr} - \omega_{0\_\rm sgl})\tau_{\rm s} + 1]} \times \frac{1}{[-i(\omega_{0\_\rm ctr} - \omega_{0\_\rm sgl})\tau_1 + 1]}, \quad (9)$$

$$\eta^{\rm CH}_{\rm ctr\_sgl} = \varepsilon_{\rm T} g_{\rm s\_sgl}(1 - i\alpha_{\rm T}) \times \frac{1}{[-i(\omega_{0\_\rm ctr} - \omega_{0\_\rm sgl})\tau_{\rm h} + 1]} \times \frac{1}{[-i(\omega_{0\_\rm ctr} - \omega_{0\_\rm sgl})\tau_1 + 1]}, \quad (10)$$

and

$$\eta^{\rm SHB}_{\rm ctr\_sgl} = \varepsilon_{\rm SHB} g_{\rm s\_sgl}(1 - i\alpha_{\rm SHB}) \times \frac{1}{[-i(\omega_{0\_\rm ctr} - \omega_{0\_\rm sgl})\tau_1 + 1]}, \quad (11)$$

represent the contributions from carrier depletion (CD), carrier heating (CH), and spectral hole burning (SHB) respectively, where

$$g_{\rm s\_sgl} = G_{\rm s\_sgl}/(1 + P_{\rm a}/P_{\rm sat}), \quad (12)$$

$P_{\rm a}$ is average power of signal pulse, $P_{\rm sat}$ is saturation power of material, and $G_{\rm s\_sgl}$ is small-signal gain. The meanings and values of other parameters can be found in Ref. [10].

Assume that input pulse is ideal soliton pulse. When the three pulses enter into SOA, Adjust the time delayed between clockwise signal pulse and control pulse $T_{\rm d}$, and then the time delayed between counter clockwise pulse and control pulse is $T_{\rm d} - T_{\rm off}$, where $T_{\rm off} = 2\Delta x/v_{\rm g}$, $v_{\rm g}$ is the group velocity of light propagating in fiber. The output signal is

$$P_{\rm B}(T_{\rm d}) = |A_{\rm CW} - A_{\rm CCW}|^2, \quad (13)$$

and the average output power is

$$P_{\rm av\_B}(T_{\rm d}) = \frac{1}{T}\int_{-T/2}^{+T/2} P_{\rm B}(T_{\rm d})\mathrm{d}t, \quad (14)$$

where T is the period of the signal pulse. The switching window and power of output signal can be obtained by solving Eqs. (5)−(7) using Runge-Kutta method.

There are three key properties to describe the performance of TOAD, which are flatness of the switching window, chirp of output pulse and the extinct ratio of the demultiplexed signal. They can be treated as following.

Flatness of the switching window: The switching window of TOAD can be obtained by changing $T_{\rm d}$. We defined four states for TOAD according to the normalized switching window, which are "off" state, "turn on" state, "on" state and "turn off" state respectively (see Fig. 2). Points A and D in Fig. 2 are decided when the normalized average output power ($P_{\rm av\_B}$) increases to 0.1. When normalized $P_{\rm av\_B}$ reaches to 80% of the maximum value in the heading part of the switching window (Point B in Fig. 2), the TOAD would be regarded as having reached the "on" state. When the normalized $P_{\rm av\_B}$ decreases to 80% of the maximum value in the tailing part of the switching window (point C in Fig. 2), the TOAD shifts to the "turn off" state. In order to describe the flatness of switching window, we define it as

$$F_{\rm sw} = 1 - \mathrm{std}[(P_{\rm av\_B})_{\rm on}], \quad (15)$$

where std$[(P_{\rm av_B})_{\rm on}]$ is the standard deviation of the normalized average output power when the TOAD in the "on" state. The bigger the $F_{\rm sw}$, the flatter the switching window.

Chirp of the output signal pulse: The maximum frequency change of the output signal pulse is calculated to describe the chirp induced by TOAD in the condition that the input signal pulse is precisely adjusted to the center of the switching window. The value of the maximum frequency change can largely character the chirp of the output signal pulse.

Extinct ratio of the demultiplexed signal: We calculate the extinct ratio of demultiplexed signal when TOAD used as demultiplexer for 4×10 Gb/s signal.

For the most cases, the wavelengths of control and signal pulse are different. All the calculations are under the following condition: $T_{\rm off}$=10 ps, duration of control and signal pulse is 1 ps. Figure 2 shows the switching window of TOAD. Vertical axis displays the value of average power of output signal from port B of TOAD divided by the average input power. It is shown that there are two peaks in the heading and tailing of switching window respectively. This result is largely coincident with the experimental results conducted by Kao[9]. Kao's experimental results show that the shape of the switching window when SOA works in the gain regime (injected current is 70 mA) is just like the simulated results. Another point should also be mentioned is that there is an overshot peak in the tailing of switching window.

In order to explain these three peaks, Eq. (13) can be rewritten as

$$P_{\rm B}(T_{\rm d}) = |A_{\rm CW}|^2 + |A_{\rm CCW}|^2 - 2|A_{\rm CW}||A_{\rm CCW}|\cos(\Delta\phi), \quad (16)$$

where $\Delta\phi$ is the difference of Phase changing between the clockwise and counter clockwise signal pulse. Figure 3 shows the $\Delta\phi$ of the signal pulse changes with the increase of $T_{\rm d}$ when the peak power of control pulse is 0.5 W. With the increasing of $T_{\rm d}$, $\Delta\phi$ increases first because of the saturation effect and the interaction of control and signal pulse, then reaches the maximum value, and decreases lightly because of the carrier recovery. The opposite case happens when $T_{\rm d}$ increases to 10 ps. $\cos(\Delta\phi)$ is also plotted correspondingly in Fig. 3. Because the peak power is too large, the maximum value of $\Delta\phi$ is almost larger than 2π. $\cos(\Delta\phi)$ changes more rapidly from 1 to -1 than from -1 to 1 in the heading and tailing part of the switching window. From Eq. (16), it can be easily seen that this kind of changing results in the two peaks in the heading and tailing part of the switching window.

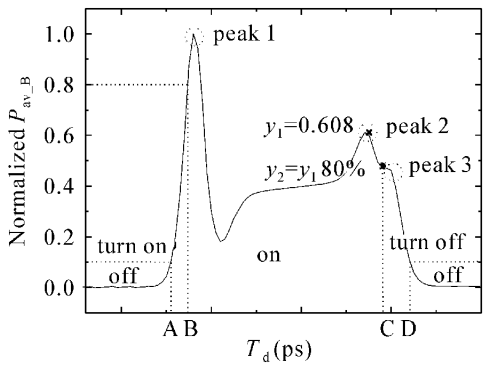

Fig. 2. Normalized switching window of TOAD ($P_{\rm ctr}$=0.5 W, $\lambda_{\rm ctr}$ = 1.55 μm, $\lambda_{\rm sig}$ = 1.55 μm).

Figure 3 also shows that there is an overshot peak in the curve of $\Delta\phi$ and $\cos(\Delta\phi)$ when $T_{\rm d}$ lies near 10 ps. It can be understand that this is the reason for the third peak in the switching window from Eq. (16). Because the existence, the transition time from "on" state to "off" state will be larger, which results in the limitation of the speed of TOAD applied as all-optical switches.

In order to obtain large output power, the wavelengths of control and signal pulse mostly should be the center of the gain spectra of SOA. In this case, the appropriate input control power is required for flat switching window.

It can be see from Fig. 4 that the switching window is relatively flat when $P_{\rm ctr}$=0.08 W. Furthermore, the output power is relatively large. It can denote that the value of $\Delta\phi$ lies close-by π, which is the main reason for the appearance of switching window.

Another measure for obtaining flat switching window is choosing appropriate wavelength of control and signal pulse. Figure 5 shows the switching window when $\lambda_{\rm ctr}$ = 1.57 μm and $\lambda_{\rm sig}$ = 1.55 μm. The corresponding $\Delta\phi$ and $\cos(\Delta\phi)$ are also plotted out. Figure 5 also indicates that the value of $\Delta\phi$ should lie close-by π in order to obtain flat switching window.

From the above interpretations, we can conclude that the value of $\Delta\phi$ should be close-by π in order to get large output power and flat switching window. There are two ways to realize this purpose. One is appropriately select the wavelengths of control and signal pulse. The other

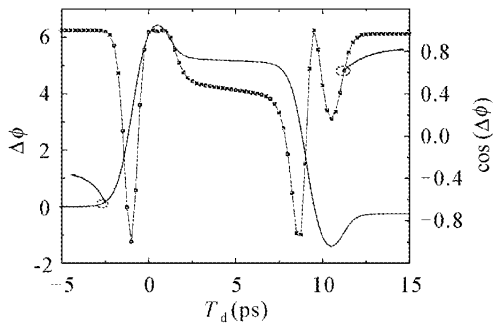

Fig. 3. $\Delta\phi$ and $\cos(\Delta\phi)$ of signal pulse when $P_{\rm ctr}$=0.5 W, $\lambda_{\rm ctr}$ = 1.55 μm, $\lambda_{\rm sig}$ = 1.55 μm.

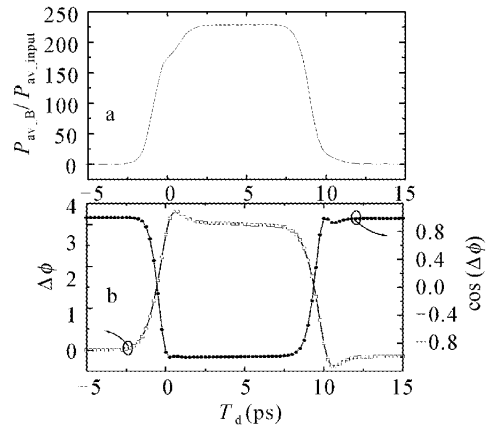

Fig. 4. Switching window of TOAD, $\Delta\phi$ and $\cos(\Delta\phi)$ of signal pulse for $P_{\rm ctr}$=0.08 W, the wavelengths of control and signal pulse are 1.55 μm. (a) Switching window; (b) $\Delta\phi$ and $\cos(\Delta\phi)$ of signal pulse.

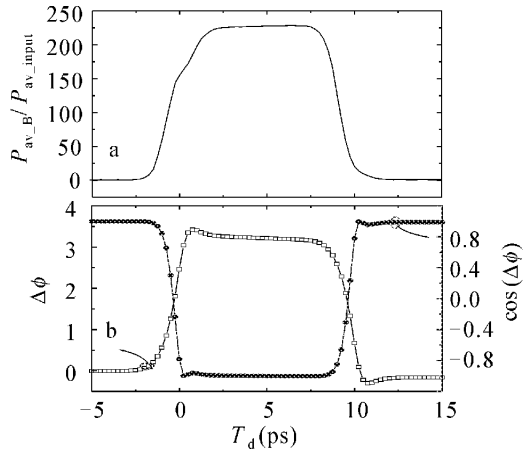

Fig. 5. Switching window of TOAD, $\Delta\phi$ and cos($\Delta\phi$) of signal pulse (P_{ctr}=0.5 W, λ_{ctr} = 1.57 μm, λ_{sig} = 1.55 μm. (a) Switching window; (b) $\Delta\phi$ and cos($\Delta\phi$).

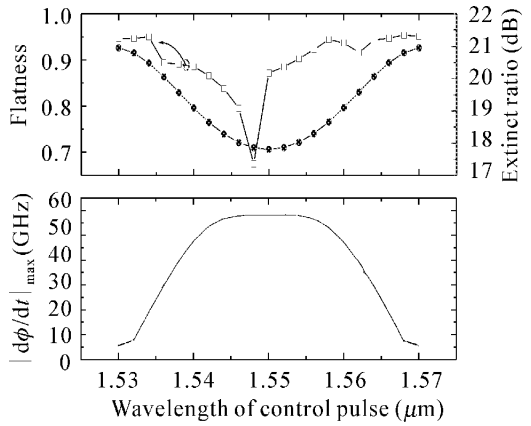

Fig. 6. Flatness of switching window, chirp of output signal, extinct ratio of demultiplexed signal of TOAD changing with the wavelength of control pulse.

is appropriately select the power of control pulse.

Figure 6 shows the Flatness of switching window, chirp of output signal, extinct ratio of demultiplexed signal of TOAD changing with the wavelength of control pulse when the wavelength of signal pulse is 1.55 μm. It denotes that when the wavelength of control pulse is in the edge of the gain spectra of SOA, the switching window becomes flat, the chirp induced by TOAD is small and the extinct ratio of demultiplexed signal is large.

Flatness of switching window, chirp of output signal, extinction ratio of demultiplexed signal of TOAD are displayed in Fig. 7 when the peak power of control pulse changes. From it we can see that when the peak power of control pulse lowers than 0.15 W, the switching window is comparatively flat and the extinct ratio is comparatively large. When the peak power of control pulse increases, the maximum frequency change decreases first, then increases with the power. It is mainly because that the chirp induced by TOAD is negative when the power of control pulse is low while the opposite happens for the high power of control pulse. The comprehensive conclusion is that the TOAD performs well when the peak power lies between 0.08 and 0.13 W.

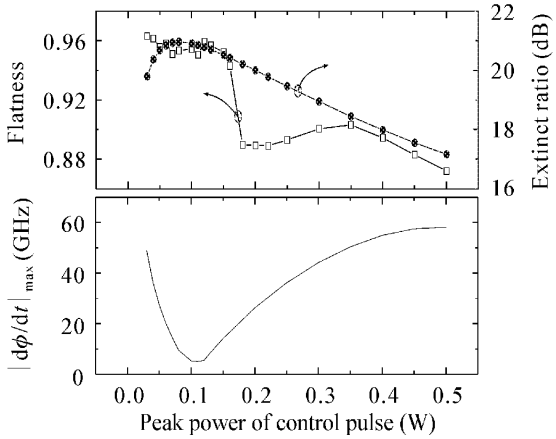

Fig. 7. Flatness of switching window, chirp of output signal, extinct ratio of demultiplexed signal of TOAD changing with the peak power of control pulse.

In conclusion, the performance of TOAD has been studied by modelling the SOA with intraband effects taken into account. Numerical results are largely coincident with the experiment results. We interpret why there are three peaks in the switching window, and put forward the definition of the flatness of the switching window of TOAD. Results show that the wavelength of signal pulse should be in the middle of the gain spectra of SOA while that of control pulse should lie in the edge of the gain spectra. Results also show that the peak power of control pulse should lie between 0.08 and 0.13 W if the wavelengths of control and signal pulse are the same.

This work was supported by the National High Technology Program of China (Grant No. 2001AA122061). L. Wen's e-mail address is weilis_wen@hotmail.com.

References

1. J. P. Sokoloff, P. R. Prucnal, I. Glesk, and M. Kane, IEEE Photon. Technol. Lett. **5,** 787 (1993).
2. R. J. Manning, A. E. Kelly, A. J. Poustie, and K. J. Blow, in *Proceedings of Nonlinear Optics '98: Materials, Fundamentals and Applications Topical Meeting* p. 159 (1998).
3. B. S. Robinson and K. K. Hall, in *Proceedings of Conference on Lasers and Electro-Optics 2000* p. 331 (2000).
4. K. L. Deng, I. Glesk, K. I. Kang, and P. R. Prucnal, IEEE Photon. Technol. Lett. **9,** 830 (1997).
5. X. Zhou, P. Ye, K. J. Guan, and J. T. Lin, IEEE Photon. Technol. Lett. **11,** 125 (1999).
6. I. Glesk, J. P. Solokoff, and P. R. Prucnal, Electron. Lett. **30,** 1322 (1994).
7. B.-Y. Yu, P. Toliver, R.-J. Runser, K.-L. Deng, D.-Y. Zhou, I. Glesk, and P. R. Prucnal, IEEE Micro. **18** (1), 28 (1998).
8. J. M. Tang, P. S. Spencer, and K. A. Shore, in *1998 IEEE Sixth International Conference on Terahertz Electronics Proceedings* p. 187 (1998).
9. Y. H. Kao, I. V. Goltser, M. N. Islam, and G. Raybon, in *Proceedings of CLEO'97* **CTuJ4,** p. 94 (1997).
10. L. S. Wen, J. Wu, and J. T. Lin, Proc. ICT **1,** 1335 (2002).
11. J. M. Tang and K. A. Shore, IEEE J. Quantum Electron. **35,** 1704 (1999).